Journal of Science: Advanced Materials and Devices 9 (2024) 100707

Contents lists available at ScienceDirect

Journal of Science: Advanced Materials and Devices

journal homepage: www.elsevier.com/locate/jsamd

Inkjet-printed multilayer structure for low-cost and efficient OLEDs

Marco Cinquino [a,b,1], Marco Pugliese [b,c,1], Carmela Tania Prontera [b,*], Fabrizio Mariano [b,c,**], Alessandra Zizzari [b], Gabriele Maiorano [b], Antonio Maggiore [b], Riccardo Manfredi [b], Chiara Mello [d], Iolena Tarantini [a], Giuseppe Gigli [a,b], Vincenzo Maiorano [b]

[a] Department of Mathematics and Physics, University of Salento, via Monteroni, Lecce, 73100, Italy
[b] CNR-NANOTEC – Institute of Nanotechnology, c/o Campus Ecotekne, Via Monteroni, Lecce, 73100, Italy
[c] Klopman International Srl, Via Armando Vona 34, Frosinone, 03100, Italy
[d] Politecnico di Torino, Corso Castelfidardo 39, Torino, 10129, Italy

ARTICLE INFO

Keywords:
Printed multilayer
OLEDs
Low-cost deposition
Inkjet-printing

ABSTRACT

Inkjet printing is considered a key technology in the fabrication of organic light-emitting diodes (OLEDs), but achieving a fully inkjet-printable OLED structure is still a challenge. Here, we propose the fabrication of OLEDs with an inkjet-printed multilayer structure (i.e. anode/hole injection layer (HIL)/electron blocking layer (EBL)/emitting layer (EML)) by properly developing new HIL and EBL inks to achieve uniform and homogeneous printed thin films. In the fabricated multilayer device, the dissolution process of the EBL, which occurs during the printing of the EML, creates a blurred interface, resulting in device performance that achieves maximum current efficiencies of 20 cd/A and 7 cd/A with ITO and printed polymeric anode, respectively. With the aim of simplifying the structure of the device and mimicking the formation of such a blurred interface, another printed multilayer structure (i.e. anode/printed HIL/printed EBL:EML) was proposed, achieving maximum current efficiencies of 13 and 6 cd/A with ITO and polymeric anode, respectively. Such results represent a compromise between simplifying the fabrication process and achieving good electro-optical properties and thus represent a further step towards the fabrication of a fully inkjet-printed ITO-free OLED.

1. Introduction

Organic light-emitting diodes (OLEDs) have attracted tremendous attention in organic electronics due to their outstanding properties, such as light weight, mechanical flexibility, high color contrast, high luminous power efficiency, low power consumption, and wide viewing angle [1–8]. Currently, they are mainly fabricated by thermal evaporation, which is a rather expensive technique with high material wastage. Solution processing techniques, particularly printing, offer a low-cost and straightforward alternative for OLED fabrication. Notably, inkjet printing is a non-contact and drop-on-demand process, and for these reasons ensures high resolution and high speed deposition with minimal material waste [9]. Nevertheless, the fabrication of a fully inkjet-printed device remains a challenging task, mainly due to the complex interplay between a large number of parameters such as viscosity, surface tensions, drying kinetics, and redissolution phenomena of the underlying layers when printing multiple layers [10,11]. In fact, despite the impressive results obtained in recent years by printing OLED layers, almost all the literature reports on the optimization of only one inkjet-printed layer of the entire device structure; in particular, the EML is the most studied. In the last decade, fluorescent emitters [12,13], phosphorescent host-guest systems [14–17], and thermally activated delayed fluorescence (TADF) materials [18–21] were successfully printed. In addition, the inkjet printing of OLED anode [22,23], HIL [24], HTL [25], electron injection layer (EIL) [26], and cathode [27] were also reported. Only a few papers dealt with the inkjet printing of a multilayer OLED structure. Lin et al. [16] reported an OLED device with an ITO anode and inkjet-printed HIL and EML, achieving a maximum current efficiency of 10.9 cd/A (Table 1). Another printed multilayer was proposed by Wang et al. [28]; in this case, four layers (from HIL to electron

Peer review under responsibility of Vietnam National University, Hanoi.
* Corresponding author.
** Corresponding author. CNR-NANOTEC – Institute of Nanotechnology, c/o Campus Ecotekne, Via Monteroni, Lecce, 73100, Italy.
E-mail addresses: tania.prontera@nanotec.cnr.it (C.T. Prontera), fabrizio.mariano@nanotec.cnr.it (F. Mariano).
[1] These Authors contributed equally.

https://doi.org/10.1016/j.jsamd.2024.100707
Received 5 January 2024; Received in revised form 5 March 2024; Accepted 10 March 2024
Available online 11 March 2024

Table 1
Literature review on printed multilayers for OLED devices.

Year	Inkjet printed layers	Max. Current Efficiency (cd/A)	Max. EQE (%)	Max. Luminance (cd/m^2)	Ref.
2019	HIL/EML	10.9	–	2192	[16]
2019	HIL/HTL/EML/ETL	55.5	14.8	1000	[28]
2020	HIL/HTL/EML	9.8	3.0	5778	[29]
2021	HIL/HTL/EML	1.62	1.15	4328	[30]
2021	HTL/EML	21.75	–	~5000	[31]
2022	HIL/HTL/EML	30.8	8.9	~5000	[32]
2023	Anode/HIL/HTL/EML	7.5	–	~3000	This work
2023	HIL/HTL/EML	20	–	~8500	This work
2023	Anode/HIL/Blend	6	–	~7000	This work
2023	HIL/Blend	13.5	–	~10,500	This work

transport layer (ETL)) were successfully inkjet-printed, achieving efficiencies above 50 cd/A with a green phosphorescent emitting material (however, this paper only describes the optimization of the ETL, without giving details on the printing of the previous layers).

In 2020, Du et al. [29] proposed an OLED structure with an inkjet-printed trilayer on a glass/ITO substrate. The peculiarity of this work is that the same material was used as both HTL and host in the EML, forming a blurred interface due to the dissolution phenomenon, which facilitated exciton formation and charge balance, thus improving the device performance. The "blurred interface" concept was exploited by the same authors for printed double or triple layers blue OLEDs [30].

In 2021, Xie et al. [31] reported an OLED structure with an inkjet-printed bilayer (HTL and EML), demonstrating the possibility of crosslinking the poly(9-vinylcarbazole) (PVK)-based HTL by using an oxidative coupling agent, to improve its solvent resistance, allowing the subsequent emissive layer to be printed. In addition, the inks used were designed to reduce the coffee ring effects and improve print uniformity.

Higher performances were recently achieved by Liu et al. [32] with an inkjet-printed trilayer consisting of poly(3,4-ethylenedioxythiophene) polystyrene sulfonate (PEDOT:PSS) as HIL, $MAPbCl_3$ as HTL, and $Ir(mpppy)_3$:mCP as a phosphorescent host-guest EML. The "blurred interface" concept between HIL and HTL was exploited to enable inkjet printing of the trilayer stack without the use of orthogonal solvents and thermal cross-linking materials.

In summary, despite the good performance achieved, the number of inkjet-printed layers in an OLED structure is still mostly limited to two or three (Table 1). It should also be noted that in no case was the anode layer printed. In fact, the reported device structures were based on an ITO anode, which makes it very difficult to scale up these architectures on flexible and unconventional substrates such as plastic or fabric, where ITO is not available or is mechanically unstable [33]. With these results in mind, we report on the inkjet printing of a multilayer OLED structure consisting of anode/HIL/EBL/EML. We first tested ITO as an anode and then compared it with an inkjet-printed PEDOT:PSS-based anode (known with the commercial name of PH1000), the printing of which was reported previously [22]. In our previous work, we also optimized the inkjet printing of an emitting layer based on a small molecule TADF on top of a spin-coated multilayer structure. Based on these results, we developed inks for HIL and EBL printing on ITO and PEDOT:PSS anodes to obtain a fully printed multilayer structure (anode/HIL/EBL/EML) for OLED devices. To simplify the printing process and the overall device architecture, another printed multilayer structure consisting of anode/HIL/EBL:EML (blend) was also tested and compared with the previous one.

The reported results demonstrate the great potential of inkjet printing for OLED fabrication and pave the way for the development of a fully inkjet-printed ITO-free OLED.

2. Materials and methods

2.1. Chemicals and reagents

5,10-Bis(4-(3,6-di-tert-butyl-9H-carbazol-9-yl)-2,6-dimethylphenyl)-5,10-dihydroboranthrene (tBuCzDBA) was purchased from Lumtec, PEDOT:PSS-PH1000 and PEDOT:PSS-AI 4083 were purchased from Heraeus Clevios™. Poly(9-vinylcarbazole) (PVK, average M_w~1,100,000, powder) and all other chemicals/solvents were purchased from Sigma-Aldrich. All chemicals were used as received without any further purification.

2.2. Ink and film characterization

The CAM 200 (KSV Instruments Ltd., Finland) instrument was used to perform pendant drop measurement and evaluate the surface tension of all solutions. The reported data are the average of three measurements with standard deviations from the medium value. The same CAM 200 apparatus was used to allow static contact angle measurements of all the solutions by the sessile drop method. Several drops of each solution were deposited onto different areas of the glass substrates and observed for 60 s, and then the respective averages and standard deviations were reported.

Film thicknesses were measured through a surface profiler (Dektak) characterized by a mechanical stylus with a 12 μm tip diameter. Ink-jet printed films were characterized by a Leica TCS SP5 confocal laser scanning microscope (Leica Microsystem GmbH, Mannheim, Germany) using a 20× dry objective and by Atomic Force Microscopy (Nanosurf EasyScan 2) in the non-contact mode using silicon tips with a nominal tip radius being less than 10 nm and WS × M was used for the image analysis.

2.3. OLEDs fabrication and characterization

Two different inkjet-printed multilayer device architecture have been exploited in this work: glass/anode/PEDOT:PSS-AI4083/PVK/tBuCzDBA/TPBi/LiF/Al and glass/anode PEDOT:PSS AI4083/PVK:tBuCzDBA/TPBi/LiF/Al. As anode, both ITO and inkjet printed PEDOT:PSS- PH1000 were used. The glass or glass/ITO substrates were cleaned with acetone and isopropyl alcohol for 10 min each and dried with nitrogen. PEDOT:PSS Clevios™ PH1000 (250 nm) was printed using a formulation described in our previous work [22]. PEDOT:PSS Clevios™ AI4083 (25 nm) was printed by dissolving the pristine solution in ethanol (PEDOT:PSS 5% in vol.), while PVK (35 nm) was printed at a concentration of 0.1 mg/mL in a solvent mixture of chloroform/ortodichlorobenzene at a ratio of 9:1 by volume. Both AI4083 and PVK were dried at room temperature for 1 min and then annealed at 120 °C for 15 and 5 min, respectively. tBuCzDBA (18 nm) was printed using a formulation described in a previous work [34]. All materials were deposited through inkjet printing using a custom-made inkjet printer fabricated by T.P.A. s.r.l. and equipped with a single nozzle having a diameter of 300 μm. For all the materials, the single nozzle printer moves at 1 m/min on the fixed glass substrate, it ejects drops with a volume of ~15 nL from a height of 7 mm above the substrate. The individual circular drops are separated by a distance of 1 mm (center to center) for every material except for PEDOT:PSS AI4083 deposited on ITO because, as shown in Fig. 1a and b, since the AI4083 drop on PH1000 is larger than that on ITO, the drop distance (center to center) during the printing has been optimized in order to have the same AI4083 thickness on both anodes, in particular, AI4083 drops on ITO are separated by a distance of 1.1 mm (center to center). For PEDOT:PSS

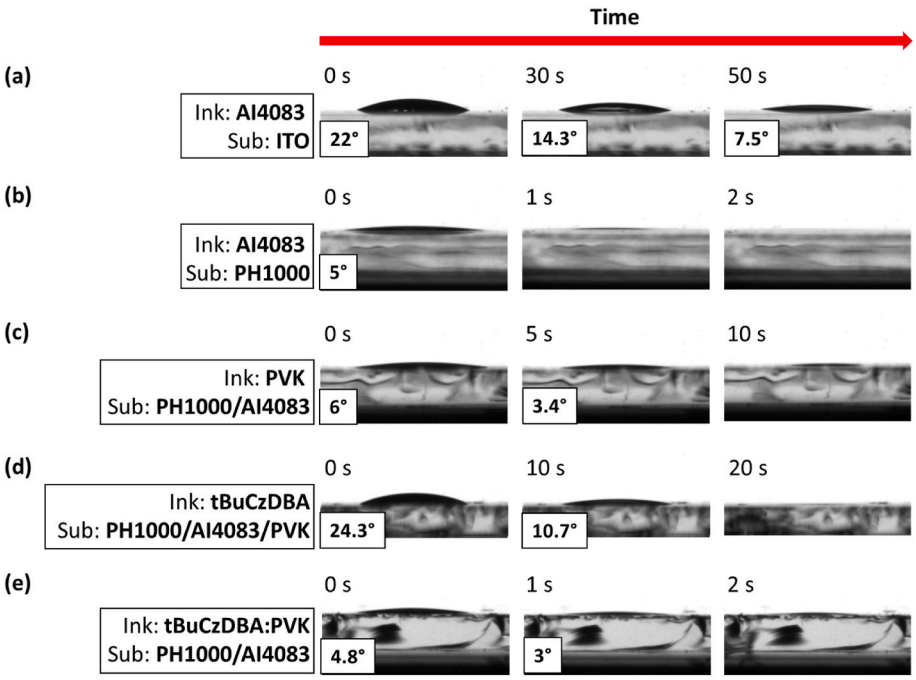

Fig. 1. Contact angles and drop drying dynamics of the developed inks: (a) AI4083 ink on ITO substrate; (b) AI4083 ink on printed PH1000 substrate; (c) PVK ink on printed PH100O/AI4083 substrate; (d) tBuCzDBA ink on printed PH1000/AI4083/PVK substrate; (e) tBuCzDBA:PVK ink on printed PH1000/AI4083.

PH1000, the final printed layers have dimensions of 13 × 24 mm^2. All the other layers have a final printed pattern with dimensions of about 3 cm^2.

Subsequently, 50 nm TPBi, 0.8 nm LiF, and 100 nm Al were deposited by thermal evaporation in a Kurt J. Lesker multiple high-vacuum chamber system. The effective light-emitting area of fabricated devices is 15 mm^2.

The optoelectronic characteristics of the OLED devices were measured in a glove box using an Optronics OL770 spectrometer coupled to the OL610 telescope unit with an optical fiber for the luminance measurements. The whole system was directly connected by an RS232 cable to a Keithley 2420 current–voltage source meter. The average device performances in terms of luminance and efficiency were calculated from the characterizations of a statistical sample consisting of 12 devices with the same structure. The overall percentage of working devices is around 90%.

3. Results and discussion

Aiming at the fabrication of a printed multilayer OLED, several inkjet-printable solutions were optimized. The target structure was as follows: anode/HIL/EBL/EML/ETL/cathode. This type of architecture was already obtained in a previous paper using ITO as the anode, a spin-coated PEDOT:PSS AI4083 as HIL, a spin-coated PVK as EBL, inkjet printed 5,10-Bis(4-(3,6-di-tert-butyl-9H-carbazol-9-yl)-2,6-dimethylphenyl)-5,10-dihydroboranthrene (tBuCzDBA) as EML, and thermally evaporated ETL (2,2′,2′′-(1,3,5-Benzinetriyl)-tris(1-phenyl-1-H-benzimidazole), TPBi) and cathode (LiF/Al) [34]. This work aims to demonstrate the possibility of obtaining a multilayer structure, up to the emissive layer, entirely fabricated by a printing process. In this context, the use of printable polymeric electrodes is particularly advantageous, as already demonstrated [22]. Therefore, the multilayer structure has been deposited both on commercial ITO and on a printed polymeric anode whose deposition process was already optimized [22]. Here, the development of new HIL and EBL ink formulations for inkjet printing is reported, while the emissive layer tBuCzDBA is deposited according to the recipe reported in our previous work [34].

The most critical aspect to evaluate in the development of a printed multilayer is the ability of the different inks to adequately wet the underlying layer and to ensure uniform deposition of the material, without causing any damage. As a first step, a PEDOT:PSS-based ink was formulated as a HIL, starting from a commercial aqueous solution (AI4083). Taking into account what has already been reported for the printing of the polymeric anode [22], the commercial solution was diluted and its surface tension was modified to obtain a value suitable for inkjet printing. In particular, the dilution with a solvent compatible with the starting aqueous solution is essential to avoid nozzle clogging and to ensure the desired thickness, while the reduction of the surface tension is necessary to ensure a low contact angle and thus a good and uniform deposition process. Following these considerations, ethanol (EtOH) was chosen as the solvent for the dilution process (95:5 EtOH: AI4083), resulting in a final formulation with a surface tension of 22.5 ± 0.8 mN/m. The contact angle of this formulation was measured on both the ITO and printed polymeric anode and the results are shown in Fig. 1a–b. As can be seen, the solution behaves very differently on the two substrates. On ITO, the initial contact angle is approximately 22°, and this ink spreads slowly until it reaches a contact angle of approximately 7.5° after 50 s. The printed polymeric anode layer, on the other hand, is much more wettable and the contact angle of the HIL formulation reaches around 5° immediately after the drop release. Despite the different behaviour, the final contact angles achieved by the two formulations are comparable and sufficiently low to ensure a good printing result and uniformity in both cases. Considering that, as shown in Fig. 1a and b, the AI4083 drop is larger on PH1000 than ITO, the drop spacing (center to center) during printing was optimized (specifically, 1.1 mm and 1 mm for ITO and PH1000, respectively) to have the same AI4083 thickness on both anodes. It can be concluded that a small contact angle combined with the low boiling point co-solvent induces a higher evaporation rate, reducing the possibility of the solute moving from the centre to the edge of the droplet. Consequently, a low contact angle is essential to reduce the coffee ring and to improve the uniformity of the thin film [31].

All the samples were characterized using a profilometer and an atomic force microscope (AFM). In both cases, a thickness of approximately 25 nm was achieved for the HIL layer and no significant differences were observed between the HILs printed on the two different

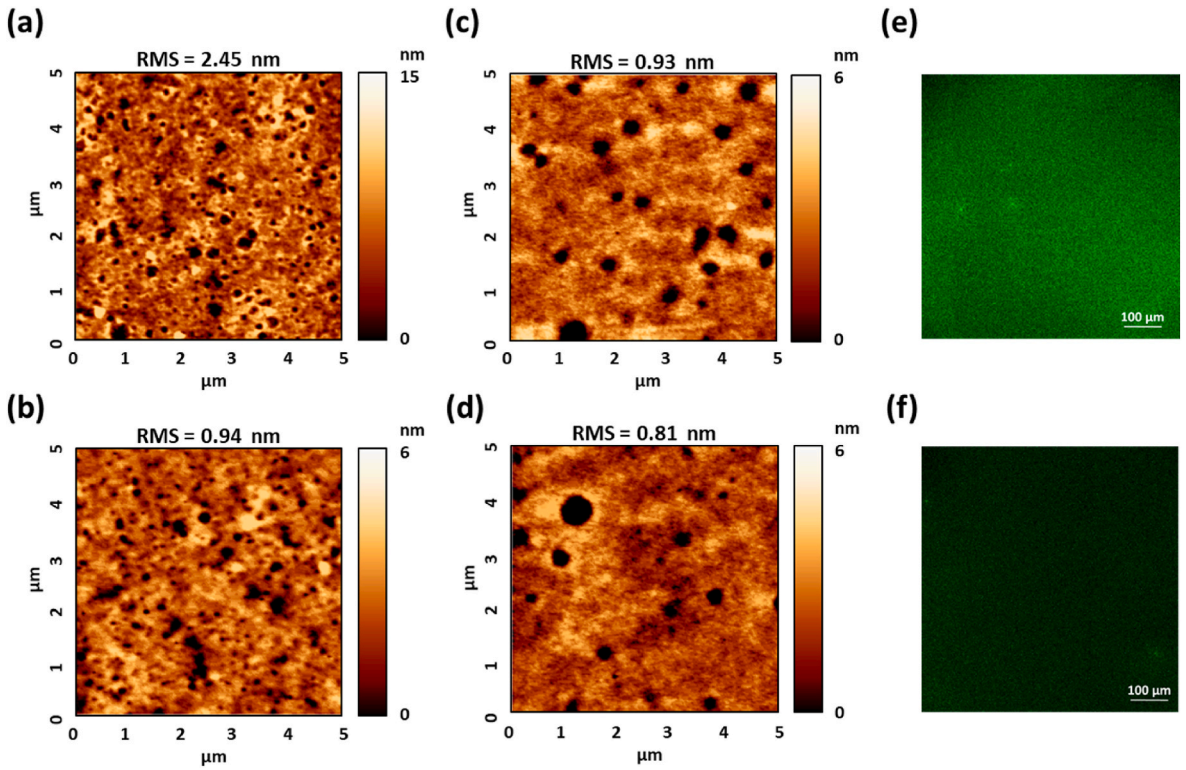

Fig. 2. Microscopic characterization of the different printed layers: (a) AFM image of printed AI4083; (b) AFM image of printed PVK; (c) AFM image of printed tBuCzDBA; (d) AFM image of printed tBuCzDBA:PVK; (e) confocal image of printed tBuCzDBA; (f) confocal image of printed tBuCzDBA:PVK.

Table 2
Roughness parameters of the printed OLED layers.

Layer	Root Mean Square (Rms, nm)	Maximum Peak Height (Sp, nm)	Maximum Pit Height (Sv, nm)
Printed AI4083	2.45	33.7	−12
Printed PVK	0.94	5.42	−9.42
Printed tBuCzDBA	0.93	5.42	−7.71
Printed tBuCzDBA: PVK	0.81	4.28	−9.42

anodes. A representative AFM image of the inkjet-printed HIL is shown in Fig. 2a. A Root Mean Square (RMS) roughness value of 2.45 nm was measured, although there are some small and evenly distributed imperfections on the thin film surface. The maximum peak height (Sp) and maximum pit depth (Sv) values of the printed HIL were also evaluated (Table 2) and were found to be in the order of tens of nanometres, making them compatible with the OLED device manufacturing process without affecting their proper functioning due to short circuits. The PVK-based EBL printing process was then performed on the printed HIL. The polymer was first dissolved in ortho-dichlorobenzene (OCB) and then diluted with chloroform ($CHCl_3$) to lower the boiling point of the solution, reduce the surface tension of the ink and create a surface tension gradient within the solution. This gradient induces Marangoni flows, thus improving the drying process of the solution and the uniformity of the layer [34]. This approach to ink formulation and printing optimization was already discussed for tBuCzDBA active layer printing [34] and we successfully applied the same concept for PVK films. Specifically, the EBL ink consists of 0.1 mg/ml PVK dissolved in a 9:1 $CHCl_3$: OCB solvent mixture, resulting in a surface tension of 25.6 ± 0.8 mN/m. The contact angle of the EBL on top of the printed HIL is shown in Fig. 1c; as can be seen, the ink spreads rapidly and is completely dry after 10 s.

The morphology of the printed film was evaluated by performing AFM measurements (Fig. 2b) and, despite some small imperfections, the roughness parameters of the film are very low (Table 2).

Finally, the emitting layer was deposited on the PVK film using an ink with a concentration of 0.25 mg/ml of tBuCzDBA in a solvent mixture of toluene:chloroform:o-dichlorobenzene 1:28/: vol, as reported in our previous work on an analogous multilayer architecture fabricated by spin coating [34]. The surface tension of the ink is 25.5 ± 0.7 mN/m, and the contact angle measured on the anode/printed HIL/printed EBL trilayer is shown in Fig. 1d, which is in agreement with the values obtained on the spin-coated trilayer [34]. The AFM and confocal microscope images of the printed layer are shown in Fig. 2c and e. The low roughness values (Table 2) and the uniform emission demonstrate the good results of the printing process. The printed multilayer, consisting of anode/HIL/EBL/EML, was then tested in an OLED structure.

To simplify the device structure and the manufacturing process, the printing of a blend consisting of PVK and tBuCzDBA on top of the HIL was developed. This printing process and the associated in-device testing are interesting because we previously demonstrated that a printed tBuCzDBA on a PVK film induces the formation of a blurred interface and an in-situ blend, which turns out to be advantageous in terms of device performance [34]. For this reason, a blend of tBuCzDBA: PVK was deposited directly on the printed HIL to test such a simplified multilayer in an OLED device. The blend was printed starting from a solution with a total concentration of 0.35 mg/ml, with a PVK: tBuCzDBA ratio of 0.4 (0.1:0.25). The same solvent combination used for tBuCzDBA printing was used to prepare this ink without any significant change in the droplet behaviour of the solution. The ink obtained has a surface tension of 26.6 ± 1.1 mN/m and the contact angles on the printed HIL are shown in Fig. 1e. The ink spreads rapidly on the HIL surface and dries evenly.

The good quality of this layer can be seen from both the AFM

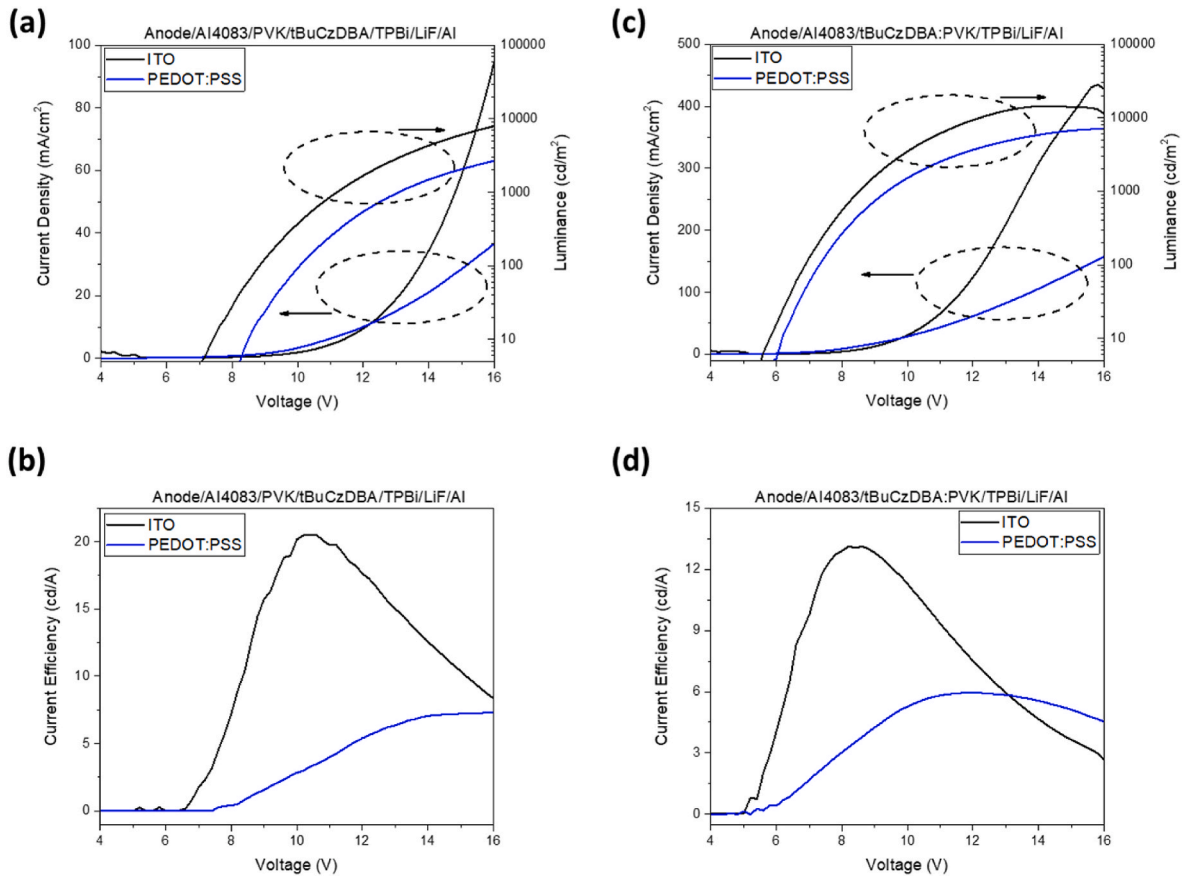

Fig. 3. Electro-optical characterization of the printed multilayer OLED devices: (a) current density vs voltage and luminance vs voltage curves for anode/AI4083/PVK/tBuCzDBA/TPBi/LiF/Al device; (b) current efficiency vs voltage for anode/AI4083/PVK/tBuCzDBA/TPBi/LiF/Al device; (c) current density vs voltage and luminance vs voltage curves for anode/AI4083/PVK:tBuCzDBA/TPBi/LiF/Al device; (d) current efficiency vs voltage for anode/AI4083/PVK:tBuCzDBA/TPBi/LiF/Al device.

Table 3
Luminance and Current Efficiency values of OLED devices with printed multilayer.

Anode	Active Layer	Max. Lum. best device (cd/m^2)	Max. Curr. Eff. best device (cd/A)	Max. Average Lum. (cd/m^2)	Max. Average Curr. Eff. (cd/A)
ITO	PVK/ tBuCzDBA	7929	20.5	6632 ± 1454	17.6 ± 4.1
PEDOT: PSS	PVK/ tBuCzDBA	2687	7.3	3234 ± 773	7.1 ± 0.5
ITO	PVK: tBuCzDBA	14418	13.1	15336 ± 1313	10.9 ± 2.4
PEDOT: PSS	PVK: tBuCzDBA	7105	5.95	7416 ± 440	5.1 ± 1.2

characterization and the confocal microscope image (Fig. 2d and f). As for the PVK/tBuCzDBA bilayer, the fluorescence of the blend film is very uniform, demonstrating the good distribution of the active material over the substrate, although the emission intensity is lower compared to a pure tBuCzDBA film because tBuCzDBA is dispersed in PVK.

The two types of printed multilayer structures (HIL/PVK/tBuCzDBA and HIL/PVK:tBuCzDBA) were tested in an OLED device on both printed polymeric anode and on ITO. The devices were completed by thermal evaporation deposition of TPBi as ETL and LiF/Al as a cathode. The results for the best devices with PVK/tBuCzDBA bilayer are shown in Fig. 3a–b, while the average performance is given in Table 3.

The ITO-based device shows a current density of 95 mA/cm^2 at 16 V and a luminance of almost 8000 cd/m^2 at the same voltage with a maximum current efficiency (CE) reaching 20.5 cd/A at 10.4 V. The switch-on voltage of this device is about 7 V. The same device prepared by using the printed PH1000 anode shows a higher turn-on voltage (about 8 V) and lower CE, luminance and maximum current density. Nevertheless, luminance values of 2700 cd/m^2 at 16 V and maximum CE values of about 7 cd/A were achieved.

As just shown, we found that OLEDs fabricated with the PH1000 polymer anode have lower performance than those fabricated on ITO. We attribute this behaviour primarily to a lower electrical conductivity of PH1000 compared to ITO, which is confirmed by a lower current density and a higher turn-on voltage. Furthermore, the ink formulation based on PH1000 requires the addition of some additives (Triton X100, see Ref. [22]) for a good filmability. As a result, the electrical and physical properties of the film can be further altered, which can influence the device performance.

Although the use of the polymeric anode is associated with a reduction in device performance, this option is particularly interesting from the perspective of fabricating a fully printed structure compatible with flexible substrates at a lower manufacturing cost. The average performance of the devices is in line with the electro-optical curve, shown in Fig. 3a–b.

Regarding the devices with PVK:tBuCzDBA blend as an active layer (Fig. 3c–d and Table 3), comparing the ITO-based and the PH1000-based OLEDs, the same differences as observed for the previous devices are noticeable, i.e. higher turn-on voltage and lower current density, luminance and CE values for the polymeric anode-based device. The best ITO anode device achieves a luminance of 11400 cd/m^2 at 16 V and a maximum CE of 13 cd/A at 8 V. In comparison, the best PH1000 anode device has a luminance of 7100 cd/m^2 at 16 V and a maximum CE of 6

cd/A at 12 V. As in the previous case, this difference is due to the lower conductivity of the polymeric anode compared to ITO. Again, the average performance is in line with the best-performing devices.

Comparing bilayer and blend devices, the latter have a lower turn-on voltage, higher current densities and luminance values, and overall lower current efficiencies. The lower turn-on voltage is due to the different device structure; unlike the bilayer one, where the PVK layer acts as a resistance for the injection of holes into the emissive layer, in the blend-based devices, the emissive layer is in contact with the HIL and the holes reach the emissive layer directly. At the same time, the absence of a PVK film as an EBL induces an increased free electrons flow, resulting in an increase in current density due to charge imbalance, with a consequent reduction in efficiency, despite the slight increase in luminance values.

In view of the reported results, the blend-based active layer OLED structure could represent a good compromise between the cost-effectiveness of the production process and the electro-optical performance of the devices.

4. Conclusion

The results presented report the fabrication of a multilayer inkjet-printed OLED. Starting from the polymeric anode up to the tBuCzDBA active layer, OLEDs were fabricated in air, without masks, overcoming/limiting the requirement orthogonal solvents. In fact, we successfully increased the number of subsequent printed layers by developing HIL and EBL ink formulations. The optimized inks allowed us to obtain uniform and homogeneous thin films and a multilayer inkjet-printed ITO-free OLED with a maximum CE of 7.5 cd/A and a maximum luminance of 3000 cd/m^2.

A simplified multilayer OLED device is also proposed by depositing a mixture of tBuCzDBA and PVK directly on the printed anode/printed HIL. The result was a device with a maximum CE slightly lower than the previous one (6 cd/A) but with a higher maximum luminance (7000 cd/m^2). The inkjet-printed multilayer OLEDs reported here are a promising starting point for the development of fully printed ITO-free OLEDs.

Declaration of competing interest

The authors declare that they have no known competing financial interests or personal relationships that could have appeared to influence the work reported in this paper.

Acknowledgements

This work was supported by: “ECOTEC” project - “ECO-sustainable and intelligent fibers and fabrics for TEChnic clothing” PON «R&I» 2014–2020, project N° ARS01_00951, CUP B66C18000300005; “TECNOMED - Tecnopolo per la medicina di precisione” - Regione Puglia: DGR n. 2117 del 21/11/2018, CUP: B84I18000540002; PNRR MUR project “NQSTI” (PE0000023); PNRR MUR project “I–PHOQS” - IR0000016; the Italian Ministry of Research (MUR) under the complementary actions to the NRRP (PNC0000007) “Fit4MedRob - Fit for Medical Robotics” Grant (contract number CUP B53C22006960001).

References

[1] R.H. Friend, R.W. Gymer, A.B. Holmes, J.H. Burroughes, R.N. Marks, C. Taliani, D. D.C. Bradley, M. Lo, W.R. Salaneck, D.A. Dos Santos, J.L. Bre, Electroluminescence in conjugated polymers, Nature (1999) 121–128, https://doi.org/10.1038/16393.

[2] P.Y. Chen, C.C. Chen, C.C. Hsieh, J.M. Lin, Y.S. Lin, Y. Lin, High resolution organic light-emitting diode panel fabricated by ink jet printing process, in: Dig. Tech. Pap. - SID, Int. Symp., 2015, pp. 1352–1354. https://doi/10.1002/sdtp.10123.

[3] Y. Kajiyama, K. Kajiyama, H. Aziz, Maskless RGB color patterning of vacuum-deposited small molecule OLED displays by diffusion of luminescent dopant molecules, Opt Express 23 (2015) 16650, https://doi.org/10.1364/oe.23.016650.

[4] N. Sain, D. Sharma, P. Choudhary, A review paper on: organic light-emitting diode (OLED) technology and applications, Int. J. Eng. Appl. Sci. Technol. 4 (2020) 587–591, https://doi.org/10.33564/ijeast.2020.v04i11.103.

[5] A.M. Bagher, Quantum dot display technology and comparison with OLED display technology, Int. J. Adv. Res. Phys. Sci. 4 (2017) 48–53. www.arcjournals.org.

[6] A. Salehi, X. Fu, D.H. Shin, F. So, Recent advances in OLED optical design, Adv. Funct. Mater. 29 (2019) 1808803, https://doi.org/10.1002/adfm.201808803.

[7] S.J. Zou, Y. Shen, F.M. Xie, J. De Chen, Y.Q. Li, J.X. Tang, Recent advances in organic light-emitting diodes: toward smart lighting and displays, Mater. Chem. Front. 4 (2020) 788–820, https://doi.org/10.1039/C9QM00716D.

[8] D. Volz, M. Wallesch, C. Fléchon, M. Danz, A. Verma, J.M. Navarro, D.M. Zink, S. Bräse, T. Baumann, From iridium and platinum to copper and carbon: new avenues for more sustainability in organic light-emitting diodes, Green Chem. 17 (2015) 1988–2011, https://doi.org/10.1039/c4gc02195a.

[9] B.M. Singh, H.M. Haverinen, P. Dhagat, G.E. Jabbour, Inkjet printing — process and its applications, Adv. Mater. 90014 (2010) 673–685, https://doi.org/10.1002/adma.200901141.

[10] C.W. Sele, T. von Werne, R.H. Friend, H. Sirringhaus, Lithography-free, self-aligned inkjet printing with sub-hundred-nanometer resolution, Adv. Mater. 17 (2005) 997–1001, https://doi.org/10.1002/adma.200401285.

[11] S. Nau, C. Wolf, K. Popovic, A. Blümel, F. Santoni, A. Gagliardi, A. di Carlo, S. Sax, E.J.W. List-Kratochvil, Inkjet-printed resistive switching memory based on organic dielectric materials: from single elements to array technology, Adv. Electron. Mater. 1 (2015) 1400003, https://doi.org/10.1002/aelm.201400003.

[12] C. Amruth, M.Z. Szymański, B. Łuszczyńska, J. Ulański, Inkjet printing of super yellow: ink formulation, film optimization, OLEDs fabrication, and transient electroluminescence, Sci. Rep. 9 (2019) 1–10, https://doi.org/10.1038/s41598-019-44824-w.

[13] L. Zhou, L. Yang, M. Yu, Y. Jiang, C. Liu, W. Lai, W. Huang, Inkjet-printed small-molecule organic light-emitting diodes : halogen-free inks , printing optimization , and large-area patterning inkjet-printed small-molecule organic light-emitting diodes : halogen-free inks , printing optimization , and large-area, ACS Appl. Mater. Interfaces 9 (2017) 40533–40540, https://doi.org/10.1021/acsami.7b13355.

[14] Y.J. Kang, R. Bail, C.W. Lee, B.D. Chin, R. Bail, C.W. Lee, B.D. Chin, Inkjet printing of mixed-host emitting layer for electrophosphorescent organic light-emitting diodes, ACS Appl. Mater. Interfaces 11 (2019) 21784–21794, https://doi.org/10.1021/acsami.9b04675.

[15] C. Kant, S. Mahmood, M. Katiyar, Large-area inkjet-printed OLEDs patterns and tiles using small molecule phosphorescent dopant, Adv. Mater. Technol. 8 (2023) 2201514, https://doi.org/10.1002/admt.202201514.

[16] T. Lin, X. Sun, Y. Hu, W. Mu, Y. Sun, D. Zhang, Z. Su, B. Chu, Z. Cui, Blended host ink for solution processing high performance phosphorescent OLEDs, Sci. Rep. 9 (2019) 1–9, https://doi.org/10.1038/s41598-019-43359-4.

[17] D.G. Yoon, Y.J. Kang, R. Bail, B.D. Chin, Interfaces and pattern resolution of inkjet-printed organic light-emitting diodes with a novel hole transport layer, J. Infect. Dis. 22 (2021) 91–98, https://doi.org/10.1080/15980316.2020.1866090.

[18] H. Wei, Y.-Q.-Q. Yi, Y. Song, L. Xie, Y. Liu, Z. Wei, Q. Dai, X. Meng, W. Su, Z. Cui, Molecularly engineered host materials for high performance inkjet-printed thermally activated delayed fluorescence organic light-emitting diodes, J. Mater. Chem. C 11 (2023) 4342–4350, https://doi.org/10.1039/D2TC05322E.

[19] A. C, B. Luszczynska, M.Z. Szymanski, J. Ulanski, K. Albrecht, K. Yamamoto, Inkjet printing of thermally activated delayed fluorescence (TADF) dendrimer for OLEDs applications, Org. Electron. 74 (2019) 218–227, https://doi.org/10.1016/j.orgel.2019.07.011.

[20] A. Verma, D.M. Zink, C. Fléchon, J. Leganés Carballo, H. Flügge, J.M. Navarro, T. Baumann, D. Volz, Efficient, inkjet-printed TADF-OLEDs with an ultra-soluble NHetPHOS complex, Appl. Phys. Mater. Sci. Process 122 (2016) 1–5, https://doi.org/10.1007/s00339-016-9726-2.

[21] C.M. Cole, S. V Kunz, T. Baumann, J.P. Blinco, P. Sonar, C. Barner-Kowollik, S. D. Yambem, Flexible ink-jet printed polymer light-emitting diodes using a self-hosted non-conjugated TADF polymer, Macromol. Rapid Commun. 44 (2023) 2300015, https://doi.org/10.1002/marc.202300015.

[22] M. Cinquino, C.T. Prontera, A. Zizzari, A. Giuri, M. Pugliese, R. Giannuzzi, A. G. Monteduro, M. Carugati, A. Banfi, S. Carallo, A. Rizzo, A. Andretta, G. Dugnani, G. Gigli, V. Maiorano, Effect of surface tension and drying time on inkjet-printed PEDOT:PSS for ITO-free OLED devices, J. Sci. Adv. Mater. Devices (2021) 100394, https://doi.org/10.1016/j.jsamd.2021.09.001.

[23] L. Kinner, S. Nau, K. Popovic, S. Sax, I. Burgués-Ceballos, F. Hermerschmidt, A. Lange, C. Boeffel, S.A. Choulis, E.J.W. List-Kratochvil, Inkjet-printed embedded Ag-PEDOT:PSS electrodes with improved light out coupling effects for highly efficient ITO-free blue polymer light emitting diodes, Appl. Phys. Lett. 110 (2017) 101107, https://doi.org/10.1063/1.4978429.

[24] C. Feng, X. Zheng, R. Xu, Y. Zhou, H. Hu, T. Guo, J. Ding, L. Ying, F. Li, Highly efficient inkjet printed flexible organic light-emitting diodes with hybrid hole injection layer, Org. Electron. 85 (2020) 105822, https://doi.org/10.1016/j.orgel.2020.105822.

[25] Y. Pan, H. Liu, S. Wang, X. Han, X. Li, Inkjet-printed alloy-like cross-linked hole-transport layer for high-performance solution-processed green phosphorescent OLEDs, J. Mater. Chem. C 9 (2021) 12712–12719, https://doi.org/10.1039/d1tc02456f.

[26] C. Amruth, B. Luszczynska, W. Rekab, M.Z. Szymanski, J. Ulanski, Inkjet printing of an electron injection layer: new role of cesium carbonate interlayer in polymer oleds, Polymers 13 (2021) 1–16, https://doi.org/10.3390/polym13010080.

[27] H. Yoon, S. Jeong, B. Lee, D. Kim, J. Park, Y. Hong, Lamination of inkjet-printed Ag electrodes for highly patternable and customizable polymer light-emitting diodes,

Flex. Print. Electron. 8 (2023) 015005, https://doi.org/10.1088/2058-8585/acb276.

[28] S. Wang, T. Shi, N. Ai, S. Jiao, S. Iguchi, Y.-C. Wu, H. Zhou, High Efficiency Fully Inkjet Printed Multilayer OLEDs Using A Printable Organic Electronic Transport Layer, IEEE 2nd Int. Conf. Electron. Technol., 2019, pp. 431–434, https://doi.org/10.1109/ELTECH.2019.8839470, 2019.

[29] Z. Du, Z. Du, Y. Liu, X. Xing, X. Xing, T. Lin, L. Liu, L. Liu, T. Chu, T. Chu, L. Wang, D. Zhang, Z. Cui, Inkjet printing multilayer OLEDs with high efficiency based on the blurred interface, J. Phys. D Appl. Phys. 53 (2020), https://doi.org/10.1088/1361-6463/ab86e1.

[30] F. Yu, Y. Wang, R. Xia, Y. Jian, L. Liu, T. Chu, Z. Wang, Z. Liu, D. Zhang, Z. Cui, A triple layer printed blue OLED with blurred interface, Flex. Print. Electron. 6 (2021), https://doi.org/10.1088/2058-8585/ac0122.

[31] J. Xie, J. Piao, L. Liu, D. Chen, Y. Liu, W. Wang, K. Cao, W. Shen, S. Chen, Ink formulation of in-situ crosslinkable hole-transporting composite for multilayer inkjet-printed organic light-emitting diodes, Org. Electron. 99 (2021) 106337, https://doi.org/10.1016/j.orgel.2021.106337.

[32] L. Liu, D. Zhang, T. Chu, Y. Jian, F. Yu, Y. Wang, Q. Gao, C. Yi, Q. Zhang, L. Sun, Z. Cui, Inkjet printed organic light-emitting diodes employing organometal-halide perovskite as hole transport layer, J. Phys. D Appl. Phys. 55 (2022), https://doi.org/10.1088/1361-6463/ac3b0f.

[33] B.H. Lee, H.C. Back, S.H. Park, K. Lee, Flexible polymer electronic devices using highly conductive polyaniline electrode, in: Org. Photovoltaics X, SPIE, 2009, p. 74161F, https://doi.org/10.1117/12.825831.

[34] M. Cinquino, C.T. Prontera, A. Maggiore, A. Zizzari, M. Pugliese, F. Mariano, V. Valenzano, I.E. Palamà, R. Manfredi, G. Gigli, V. Maiorano, Toward highly efficient solution-processable OLEDs: inkjet printing of TADF emissive layer, Adv. Electron. Mater. (2023). https://onlinelibrary.wiley.com/doi/10.1002/aelm.202300358.